Vertical ladder climbing by the HRP-2 humanoid robot

Joris Vaillant, Abderrahmane Kheddar, Hervé Audren, François Keith, Stanislas Brossette, Kenji Kaneko, Mitsuharu Morisawa, Eiichi Yoshida, Fumio Kanehiro

Vertical Ladder Climbing by the HRP-2 Humanoid Robot*

Joris Vaillant[1,2], Abderrahmane Kheddar[2,1], Hervé Audren[2,1], François Keith[1,2], Stanislas Brossette[2,1], Kenji Kaneko[2], Mitsuharu Morisawa[2], Eiichi Yoshida[2], Fumio Kanehiro[2]

***Abstract*— We report the results obtained from our trials in making the HRP-2 humanoid robot climb vertical industrial-norm ladders. We integrated our multi-contact planner and multi-objective QP control as basic components. First, a set of contacts to climb the ladder is planned off-line and provided as an input for a finite state machine that sequences tasks to be realized by our multi-objective model-based QP in closed-loop control. The trials we made revealed that hardware changes are to be made on the HRP-2, and the software has to be made more robust. Yet, we confirmed that HRP-2 has power capability to climb real industrial ladders, such as those found in nuclear power plants and large scale manufacturings (e.g. airliners, shipyards and buildings).**

I. Introduction

Humanoid robots walking on flat grounds and climbing stairs have grown in maturity over the last years. The Honda's Asimo is a good illustration of such an achievement. Such maturity level is not yet observed in walking on uneven or deforming terrains, and non-gaited motion requiring whole-body multi-contact motion such as in climbing ladders.

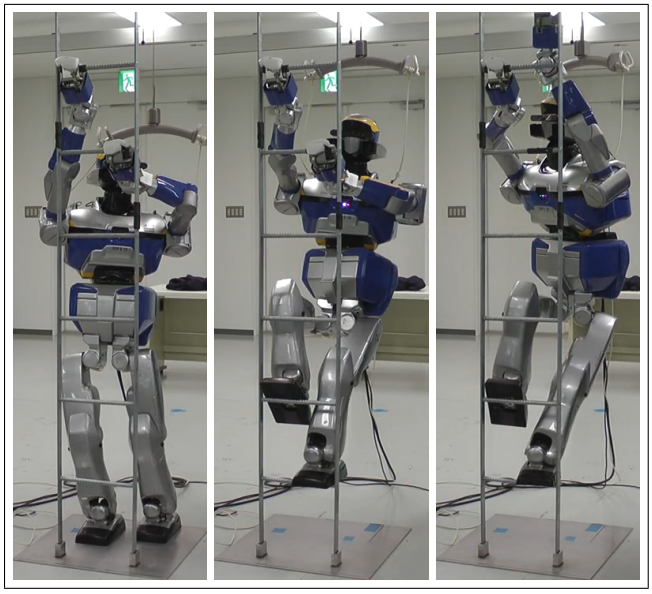

Fig. 1: HRP-2 climbing a vertical ladder. Notice: (i) Not possible to put two feet on a same rung (ii) Closed grippers cannot not grab firmly the rungs (iii) each foot can be freely positioned on rungs: the right foot is rotated to increase the reaching range of the left arm.

The DRC contest defined ladder climbing as one of the eight challenging tasks. Indeed, ladder climbing is one of the recurrent task encountered for intervention in disaster nuclear power-plants, or more generally in maintenance, dismantling or building large sites. In response to the DRC, different strategies for ladder climbing were tried out. Yet, all teams chose the most inclined 60deg ladder having rungs of 10cm width, which more closely resembles stairs. In fact, the winning SCHAFT team could climb the DRC ladder without even using its arms. The DRC-HUBO humanoid robot, based on multi-contact planning [1], could climb almost all of it [2], whereas KAIST team, also with HUBO completed the climbing. Yet, no of teams (with Atlas or own robots) succeeded in climbing the ladder.

Prior to the DARPA challenge, a number of ladder climbing customized robots were made. For example, in [3] a four prismatic arms with gripper robot was designed for nuclear power plants. In [4], a planar three legged climbing robot was demonstrated in climbing pegs; this study reveled that by identifying key motion primitives coupled with physics simulation, the planning is tractable and can be optimized according to desired criteria. Ladder climbing was also demonstrated with multi-rigid-to-soft legs robot in [5]. In [6], a six legged spider-like robot was programmed to climb successfully a vertical ladder. Interestingly, this study showed that having enough limbs would allow climbing without firm grasps, since contact formations are all of hook-like type.

In [7] a Gorilla-type robot was shown to climb a vertical ladder having in mind transitions toward multi-modal locomotion capabilities. They achieved three different climbing gaits: transverse, pace with constant velocity and trot with acceleration. This study reveled the importance in considering dynamic effects and suggested to pay particular attention to the axis of yawing. Lastly, [8] demonstrated capabilities of the HRP-2 in inclined ladder climbing (2 stairs and reaching) and took a strategy consisting in distributing contact forces and moments together with joint torques. Although they used different naming, the general approach is similar to our multi-contact strategies described in [9][10].

Our work addresses HRP-2 climbing a vertical ladder, see Fig. 1. Two main issues drive our research:
1) address vertical ladders; relatively to [7][8][2]... we use industrial norm ones: we prohibit any change or adjustment on the ladders as this would not be possible in practice.
2) use HRP-2 as it is and fully exploit its limits. The idea is to work on the software as much as possible.

The main objectives of our work are as follows:

- Evaluate our multi-contact planner and controller in the context of ladder climbing;
- Check the capability of HRP-2 to climb up and down a vertical industrial norm the ladder;
- Draw lessons for software and hardware modifications.

II. Multi-contact planner

The underpinning of our work is described in [11]. In brief, a multi-contact planner (MCP) uses the HRP-2, ladder and environment models (assumed known) to generate off-line a sequence of postures in contact to climb the ladder.

*This work is supported partly by internal grants from IS-AIST, the JSPS Kakenhi B No 25280096, and the FP7 KoroiBot.

[1]CNRS-UM2 LIRMM, Interactive Digital Human, Montpellier, France
[2]CNRS-AIST Joint Robotics Laboratory, UMI 3218, Tsukuba, Japan

For the ladder, we use nearly the parametrization in [2], whereas the robot is covered by patches of spheres and tori for smooth distance computation [12].The postures computed by the MCP are passed to a finite state machine (FSM) that will split them into subtasks so as to account for uncertainties during task execution. The FSM elaborates additional tasks and changes on-line their objectives to deal with different primitives (contact adding, grasps, contact removal, center of mass shifts, etc). These FSM tasks are passed to our multi-objective QP controller in addition to the already embedded core one (e.g. limits, collision avoidance, etc.).

There is two ways to generate climbing contact stances:

- Contact stances are automatically planned providing guidance (e.g. favoring a climbing hands/feet sequence behavior), see [10][9].
- Contact pairs and sequence are specified by the user, like in [1], to be used in teleoperation mode for example.

In both cases, a posture generator (PG) –that is a non-linear optimization formulation of a generalized inverse kinematics, seeks for viable statically stable postures that remove or add contacts as suggested by the automatic or interactive planner. The posture shall fulfill constraints of joint and torque limits, reaction forces within their friction cones, equilibrium, non-desired collisions. We may also add other secondary task constraints such as gaze or field-of-view, etc. [10][9].

Compared to [11], we brought two changes: (i) more refined contact models, and (ii) the possibility to compute postures at once (i.e. at a glance) to generate optimal postures that minimizes a given cost over the entire path.

A. Contact modeling in posture generation

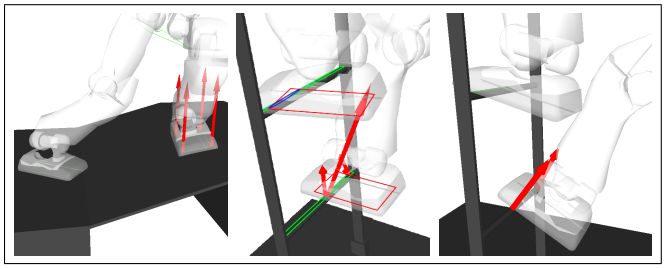

Fig. 2: Three contact models used in the posture generator.

As part of the posture generator optimization process, we have three contact models. The first predefines patches associated to each contact area, see [9][10], Fig. 2(left image). Now, we are able to generate contacts with any position and orientation without the need to use predefined contact patches, see Fig. 2(middle image), and [13] for more technical details. Finally, we also implemented contact of the form plane/cylinder to have more contact possibilities (e.g. sole/rung contact), Fig. 2(right image).

B. Global posture generation with gripper torque optimization

For N stances, we consider as if we had N robots each with own associated variables. We use the following notation in the rest of the paper:

- X_i the link i transformation matrix w.r.t the overall reference frame;
- r_i is the translation vector of link i;
- $E_i = [T_i, B_i, N_i]$ the orientation matrix and its vector components (the nomenclature of the latter is useful to handle contacts).

For N robots, $x = [\mathbf{q}_1^T, \cdots, \mathbf{q}_N^T, \mathbf{f}_1^T, \cdots, \mathbf{f}_N^T]^T$ is the optimization vector, where $\mathbf{q}_i$ is the robot i configuration vector and $\mathbf{f}_i$ the robot i contact forces vector. We use over- or sub-script i to refer to the i-th robot. Each robot must satisfy the following constraints:

• Static equilibrium: $\underline{\tau}_i \leq J^i(\mathbf{q}_i)^T \mathbf{f}_i - g^i(\mathbf{q}_i) \leq \overline{\tau}_i$, J is the Jacobian of all contact-force points and g the gravity term.

• Joint limits: $\underline{\mathbf{q}}_i \leq \mathbf{q}_i \leq \overline{\mathbf{q}}_i$, $\underline{\mathbf{q}}_i$ and $\overline{\mathbf{q}}_i$ are the upper and lower bounds for the robot i. Of course, the range of the joint limits for any i are the same for a given joint, but $\mathbf{q}$ is ordered differently for each robot i because of the change of the reference base.

• Self-collisions: $\delta(X_j^i(\mathbf{q}_i), X_k^i(\mathbf{q}_i)) > \epsilon_{jk}$, $\forall (j,k) \in \mathcal{I}^i_{\text{self}}$, δ is the distance function, and k (not successive), ϵ_{jk} is the user set minimum distance, and $\mathcal{I}^i_{\text{self}}$ the set of self-collisions to avoid on robot i.

• Other collisions: $\delta(X_j^i(\mathbf{q}_i), X_k) > \epsilon_{jk}$, $\forall (j,k) \in \mathcal{I}^i_{\text{robot-env}}$, the set of robot-environment collisions pairs to avoid at i.

• Non-sliding contacts: $\mu_j N^i(\mathbf{f}_i, j) > \|TB^i(\mathbf{f}_i, j)\|$, $\forall j \in \mathcal{I}^i_{\text{contact}}$, the set of contact points at i, μ_j is the friction at the contact point j, $N^i(\mathbf{f}_i, j)$ the j-th normal force component, $TB^i(\mathbf{f}_i, j)$ the tangent space force vector components.

• Fixed contacts (6 constraints): $r_j^i(\mathbf{q}_i) - r_k = \vec{0}$, $N_j^i(\mathbf{q}_i) \cdot T_k = 0$, $N_j^i(\mathbf{q}_i) \cdot B_k = 0$, $B_j^i(\mathbf{q}_i) \cdot T_k = 0$, $N_j^i(\mathbf{q}_i) \cdot N_k \geq 0$, $B_j^i(\mathbf{q}_i) \cdot B_k \geq 0$, where k subscript is for environment surface and j the robot surface.

• Planar contacts (5 constraints): $(r_j^i(\mathbf{q}_i) - r_k) \cdot N_k = 0$, $N_j^i(\mathbf{q}_i) \cdot T_k = 0$, $N_j^i(\mathbf{q}_i) \cdot B_k = 0$, $N_j^i(\mathbf{q}_i) \cdot N_k \geq 0$, $\text{conv}(\mathcal{P}_j) \in \text{conv}(\mathcal{P}_k)$, where $\mathcal{P}_j$ and $\mathcal{P}_k$ are the surface j and k points, conv is the convex hull.

• Cylindrical contacts (6 constraints): $w_{\min} \leq (r_j^i(\mathbf{q}_i) - r_k) \cdot T_k \leq w_{\max}$, $(r_j^i(\mathbf{q}_i) - r_k) \cdot B_k = 0$, $(r_j^i(\mathbf{q}_i) - r_k) \cdot N_k = 0$, $T_j^i(\mathbf{q}_i) \cdot B_k = 0$, $T_j^i(\mathbf{q}_i) \cdot N_k = 0$, $T_j^i(\mathbf{q}_i) \cdot T_k \geq 0$, where $w_{\min}$ and $w_{\max}$ are the width of the surface.

• Link all robots common contacts:

$$\begin{aligned} r_k^i(\mathbf{q}_i) - r_k^j(\mathbf{q}_j) &= \vec{0} \\ \text{Err}(E_k^i(\mathbf{q}_i), E_k^j(\mathbf{q}_j)) &= \vec{0} \end{aligned} \quad \forall (i,j,k) \in \mathcal{I}_{\text{common}}$$

We use the cost function $\mathcal{C} = \sum_{i=1}^{N} \mathcal{C}_i$ for each robot i:

$$\begin{aligned} \mathcal{C}_i(\mathbf{q}_i, \mathbf{f}_i) = w_q \|\mathbf{q}_i - \mathbf{q}_i^d\|^2 + \sum_{j \in \mathcal{I}_{\text{contF}}} w_j \|F(\mathbf{f}_i, j)\|^2 + \\ \sum_{j \in \mathcal{I}_{\text{contT}}} w_j \sum_{p \in \mathcal{I}_{\text{points}_j}} \|M_j \cdot (r_p \times F(\mathbf{f}_i, p))\|^2 + \\ \sum_{j \in \mathcal{I}_{\text{posT}}} w_j \|r_j^i(\mathbf{q}_i) - r_j^d\|^2 + \sum_{j \in \mathcal{I}_{\text{rotT}}} w_j \|\text{Err}(E_j^i(\mathbf{q}_i), E_j^d)\|^2 \end{aligned}$$

where Err is an implementation of several methods to compute orientation error, all $\mathcal{I}_x$ represent sets of x, all w_x are cost weights for cost part x, q_i^d is the targeted configuration vector, $F(\mathbf{f}_i, j)$ is the $\mathbf{f}_i$ j-th force vector, contF and contT are contact forces and moments respectively, M_j is the motor rotation axis vector, r_p is the motor to point p translation, $\mathcal{I}_{\text{points}_j}$ the set of contact points in contact j, posT and rotT means target positions r_j^d and orientations E_j^d respectively.

We use the Ipopt non-linear solver [14] with the RobOptim[1] framework to implement the PG.

III. Multi-objective QP controller

A. Model-based QP multi-contact controller

To control our robot, the tasks are formulated as a model-based QP that is solved at each time-step T and used in closed-loop. The optimization variables are composed by $\mathbf{x} = [\ddot{\mathbf{q}}^T, \boldsymbol{\lambda}^T]^T$ where $\ddot{\mathbf{q}}$ is the joint acceleration vector and $\boldsymbol{\lambda}$ is the linearized friction cone base weights. We refer to $\mathbf{f}$ as $K\boldsymbol{\lambda}$ where K is the discretized friction cone matrix. We do not make any distinction between the robot joint and the free-flyer coordinate except that the last one are not actuated. The QP controller writes as follows:

$$\underset{x}{\text{minimize}} \sum_{i=1}^{N} w_i \|E_i(\mathbf{q}, \dot{\mathbf{q}}, \ddot{\mathbf{q}})\|^2 + w_\lambda \|\boldsymbol{\lambda}\|^2$$

subject to

$$1)\ \underline{\tau} \leq M(\mathbf{q})\ddot{\mathbf{q}} + N(\mathbf{q}, \dot{\mathbf{q}}) - J^T\mathbf{f} \leq \overline{\tau} \qquad \boldsymbol{\lambda} \geq 0$$

$$2)\ S(J_i\ddot{\mathbf{q}} + \dot{J}_i\dot{\mathbf{q}}) = -S\frac{v_i}{T} \quad \forall i \in \mathcal{I}_{\text{contact}}$$

$$3)\ \max\left(\dot{\underline{\mathbf{q}}}, -\xi\frac{(\mathbf{q} - \underline{\mathbf{q}}) - q_s}{q_i - q_s}\right) - \dot{\mathbf{q}} \leq \ddot{\mathbf{q}}T$$

$$4)\ \ddot{\mathbf{q}}T \leq \min\left(\dot{\overline{\mathbf{q}}}, \xi\frac{(\overline{\mathbf{q}} - \mathbf{q}) - q_s}{q_i - q_s}\right) - \dot{\mathbf{q}}$$

$$5)\ \dot{\delta} + \ddot{\delta}T > -\xi\frac{\delta - \delta_s}{\delta_i - \delta_s}$$

The constraint 1) entails for torques bounds $\underline{\tau}$ and $\overline{\tau}$ using the dynamic equation in which $M(\mathbf{q})$ is the whole-body inertia matrix, $N(\mathbf{q}, \dot{\mathbf{q}})$ is the non-linear Coriolis and Gravity vector and J for the contact points Jacobian. This constraint also ensures that the contact force stays in the discretized friction cone. The constraint 2) fulfills non motion for body in contact, J_i is the translation and rotation Jacobian of the body $i \in \mathcal{I}_{\text{contact}}$. The right term writes generally as 0, but in practice, countering contact body velocity v_i (due to integration errors) leads to a more robust behavior. $S \in \mathbb{R}^{n,6}$ is a selection matrix that allows to free some contacting bodies to be controlled in impedance or admittance. The constraints 3) and 4) enforces joint speed and range limits and use a velocity damper and q_s as a security range (constraints are triggered only when $q \leq q_i$), ξ is the damping gain. The constraint 5) deals with collision avoidance and uses also a velocity damper in the same way as [15]. δ is the distance between a pair of bodies computed with the SCH library [12]. $\dot{\delta} = N^T J\dot{\mathbf{q}}$ and $\ddot{\delta} = \dot{N}^T J\dot{\mathbf{q}} + N^T(\dot{J}\dot{\mathbf{q}} + J\ddot{\mathbf{q}})$. N is the normal distance vector and $\dot{N}$ is computed by finite difference.

As for the objective function: $w_{\boldsymbol{\lambda}}$ is the weight that enforces positive definiteness of the Hessian matrix. $E_i(\mathbf{q}, \dot{\mathbf{q}}, \ddot{\mathbf{q}})$ is a quadratic task function of $\ddot{\mathbf{q}}$. For ladder climbing we only use the Set Point objective task [16][17][18] written as:

$$k_i\mathcal{T}_i - 2\sqrt{(k_i)}\dot{\mathcal{T}}_i - J_{\mathcal{T}_i}\ddot{\mathbf{q}} - \dot{J}_{\mathcal{T}_i}\dot{\mathbf{q}}$$

with $\mathcal{T}_i \in \mathbb{R}^n$ a n-dimensional task error, and $J_{\mathcal{T}_i}$ is the task Jacobian. We use the following tasks :

- Posture task: $\mathcal{T}_{\text{posture}} = \mathbf{q}_d - \mathbf{q}$
- Body i position task: $\mathcal{T}_{\text{pos}} = r_i^d - r_i(\mathbf{q})$
- Body i orientation task: $\mathcal{T}_{\text{ori}} = \text{Err}(E_i^d, E_i(\mathbf{q}))$
- Body i linear velocity task: $\mathcal{T}_{\text{linear-velocity}} = v_i^d - v_i(\mathbf{q}, \dot{\mathbf{q}})$
- CoM task: $\mathcal{T}_{\text{CoM}} = \text{CoM}_d - \text{CoM}(\mathbf{q})$

We are using the LSSOL QP solver. On a i7 2.6 GHz laptop, the median computation time of the whole problem (cost function, constraint matrix, distance query and QP solving) during ladder climbing (3 or 4 contacts) is $\approx$ 1ms.

B. Dealing with ankle shock absorbing compliance

At each HRP-2 ankle, there is a shock absorbing compliant mechanism linking the feet to the legs. It prevents the force sensor from malfunctions in the event of high impacts. Moreover, compliance (also available in both HRP-2 wrists) is important to absorb light discrepancies at contact formation/removal and has a *stabilizing effect*. Unfortunately, this compliance makes the attitude of the robot harder to control and this is the reason why a 'stabilizer' has been devised to achieve robust walks. The HRP-2 built-in stabilizer is well designed for walking on flat terrains and assumes coplanar contacts. Therefore, it has to be turned-off in climbing or any non-coplanar multi-contact motion. Since we use model-based planning and control, it is important to account for the effect of such a compliance.

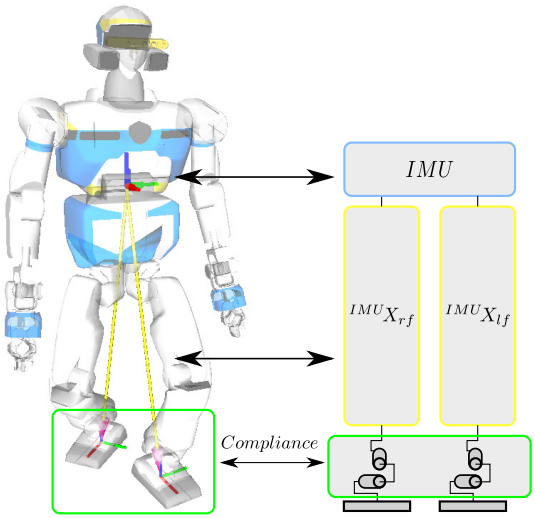

Fig. 3: Compliance kinematic model.

In order to compensate for the ankles' compliance, we estimate it using the robot embedded IMU and inverse kinematics (IK). We model each compliance as a two revolute joints at each ankle, see Fig. 3. Each leg (contact) is modeled as a fixed base with 2dof and an end effector going through the IMU. Since in our experiments, two contacts at least are necessary, we are always having at least one closed-kinematic chain between contacts. We exploit this fact to estimate the 4 joints that model the compliance effect. In the example illustrated in the Fig. 3, we considered all the open kinematic chains that go through the IMU and write, at the IMU frame, the conditions to close the kinematic chain in position, and secondary (at best) in orientation considering the lowest possible motion. The problem can be solved by optimization or prioritized task frameworks. The ground truth data we assume are, of course the joint encoders of the remaining joints, the IMU is reliable, and the type of contact.

[1] www.roboptim.net

Let $\mathbf{q}_{\text{model}}$ be the robot configuration used by the controller and $\mathbf{q}_{\text{estimate}}$ be the robot configuration that accounts for the compliance. First, we tried using the compliance estimation as a task, $\mathcal{T}_{\text{pos}}$ and $\mathcal{T}_{\text{ori}}$, where the position and the orientation error and velocity are computed from the $\mathbf{q}_{\text{estimate}}$. As a result, the robot tries fixing its position without counterbalancing the compliance's dynamics, resulting in falls or oscillations. Instead, we reduce the dynamics of the motion with the following definition of the task error (to any task $\mathcal{T}$):

$$\mathcal{T} = K_p \mathcal{T}(\mathbf{q}_{\text{model}}) + K_i \int_{T_i}^{T_e} \mathcal{T}(\mathbf{q}_{\text{estimate}}) dt$$

where $K_p \gg K_i$, T_i and T_e are the task insertion and removal times. This allows converging to a nil error with slow dynamics.

C. Gripper/rung contacts

The ankle's compliance can cause gripper/rung contact loss. To fix this issue we implemented a simple force control. This is made possible since we can release the null velocity constraint on a chosen axis (see selection matrix S in section III-A). When the force goes below f_{c_σ} we remove the null velocity constraint on the insertion axis of the gripper's (z-axis) and add a position task with high weight. The targeted position is as follows:

$$z_{\text{target}} = z_{\text{init}} + \min(\kappa(f_{c_\sigma} - f_c), z_{\max})$$

z_{init} is the initial position of the contact, $z_{\max}$ is the maximum displacement of the contact, κ is a unit converting gain.

IV. Experiments and Results

A. Simulated scenarios

Although the focus of this paper is on assessing HRP-2 humanoid robot climbing up and down vertical industrial-norm ladders, we achieved simulations with transitions to scaffolding, and the DARPA dimensions inclined ladder.

Fig. 4 illustrates the result of a simulated scenario for which a real set-up is already available at our AIST experimental room. Our mid-term goal is to achieve a complete multi-modal locomotion where the robot walks to the ladder, climbs it up to a scaffolding and then stands on the scaffolding to walk somewhere else and come back. Assuming firm grasps are possible on rungs and stringers, the planner can take advantage of those rungs and stringers to achieve its goal. More importantly, multi-contact planner also found transition strategies from ladder climbing to the scaffold via the narrow passage (kept with dimensions similar to those found in industry). Fig. 5 illustrates the climbing of the DRC dimension ladder (the same used in the qualifying december 2013 context), which appears somehow oversized as compared to HRP-2. Yet, HRP-2 found a multi-contact path to climb the ladder, see also in [13] examples with simulated Atlas humanoid robot.

B. Experiments with HRP-2

The ladder's parameters we use are represented on Fig. 6. The ladder is put between the gantry crane and the floor. The HRP-2 is put with a precomputed initial posture near the ladder. Since the ankles compliance is compensated in the QP, the robot can reach and grasp the first rung.

We report our results in experimenting the HRP-2 climbing up and down (by reverse plan). The first problem we face

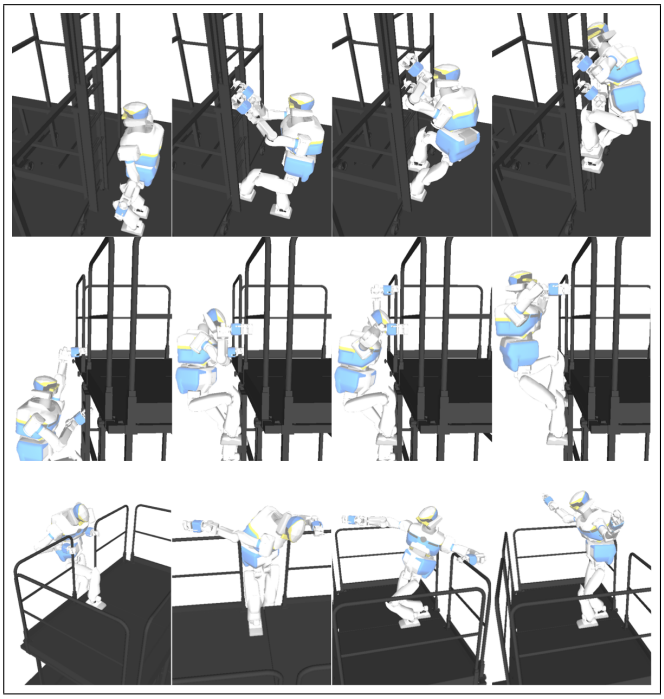

Fig. 4: HRP-2 climbing the ladder to reach a scaffolding.

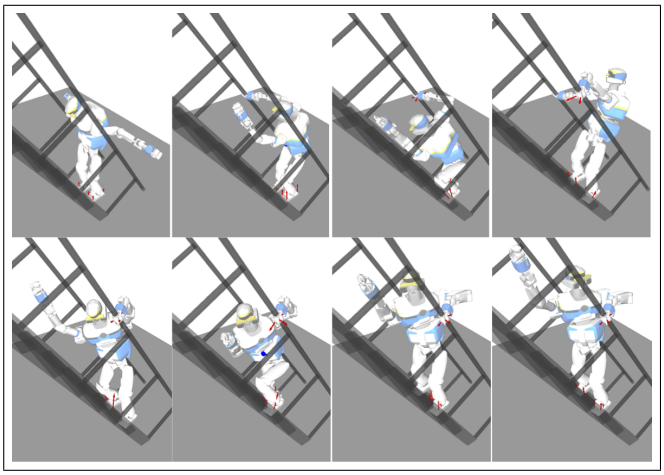

Fig. 5: Snapshot from three steps climbing of the DRC inclined ladder.

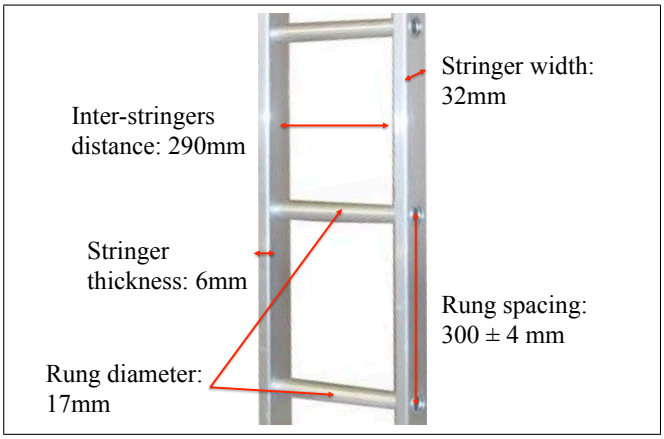

Fig. 6: Ladder parameters used in HRP-2 experiments.

is to secure the robot. The strings attaching the robot to the roof's XY-trailer are not easy to operate in these conditions. We devised an experimental methodology before real trials as follows: First, we turn off the recovery FSM assuming the contacts to occur as expected and play the entire climbing with the robot in the air. This step confirms that the motion is indeed auto-collision free and doable. Second, preliminary trials consist in playing, on the ladder, the planned simulated motion in open-loop. It is the duty of the user to close the loop by adjusting the robot when needed; see Fig. 7. This step is important (and probably not possible with powerful robots like Atlas). It confirmed that the robot could climb the ladder entirely yet with the help of the operator in some phases, namely help in sustaining grasps during one of the arm transition phase, see Fig. 7.

The third phase of the experiments consist in redesigning the planning by using only rungs and operate the ladder in *real-time closed-loop QP controller without human intervention*. Climbing up and down the ladder is provided with the accompanying multimedia video. However, it was not possible for HRP-2 to achieve the third transition of the arm to climb more than two rungs because of kinematic reaching limits, the best of what was tried to achieve a complete fully autonomous climbing is illustrated by the Fig. 1.

C. Discussions

Although the experiments show that the HRP-2 humanoid robot has the capability to climb vertical ladders, which no humanoid platform proved to achieved up-to-now, we draw lessons and issues to improve prior to experimenting larger variety of ladders with transitions to other modalities, such as the simulation in Fig. 4.

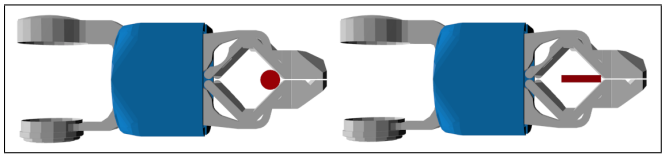

Fig. 8: Disposition of the rungs and stringers within the HRP-2 gripper once closed.

The most critical problem that our experiments revealed relates to the current HRP-2's grippers: their design limited too much the possible various climbing strategies. The Fig. 8 illustrates the disposition of a rung or a stringer once the gripper is closed around it. Notice the large gap that remains and within which the rung or the stringer is potentially free to move. The consequence of this situation are multiple. In some cases the gripper would simply open and loose the contact during one of the other arm free motion transition. This is because of the mechanical constraints: pulling forces apply at weak points of the gripper. To circumvent partly this problem, we increased temporarily the P gains of the gripper's servo motor. Indeed, this allowed maintaining the grippers close during rung grasp, but it was not enough for stringer's grasp. Subsequently, stringers were not used for the autonomous climbing experiment. Yet, experiments allowing sporadic user's intervention showed that if the stringers can be grasped firmly, the ladder climbing is less constrained and the planner can alternate and combine between stringer/rung grasps. Even if enough torques was available to maintain the gripper closed, the lack of firm grasps result in robot's attitude errors w.r.t the ladder, and kinematic reachability could be jeopardized if too much discrepancies occur. All these were observed in practice, because not only the contact points are almost coplanar, but they are nearly aligned.

Unfortunately, it appears clearly that the only possible solution consists in redesigning a new pair of grippers, which are currently being manufactured. With new grippers, wider ladder climbing experiments will be considered and the simulated walk-to-ladder-to-scaffold scenarios can then be experimented.

Compliant shock absorbing mechanisms in the ankles and also in both wrists absorb light perturbations, namely during transfer motions. Yet, they won't be able to absorb important ones. Torque controlled humanoid would comply to such perturbations nicely, but a stiff position-controlled humanoid would behave like a rock, and a perturbation means generally loosing unilateral contacts or contact sliding. For the time being the light perturbations we emulate by touch during trials do not seem critical for the climbing tasks. However, we are planning to servo the robot with low PD gains and a feedforward term $u = K_p\epsilon + K_s\dot{\epsilon} + \mathcal{D}(q,\dot{q})$: K_x being the gains, ϵ the servo position error and $\mathcal{D}$ the feedforward term. This idea was also discussed in [2], where the K_p gain was adjusted in the gripper at the cost of loosing precision, whereas $\mathcal{D}$ was left for future work.

Although HRP-2 seems already very well-designed in finding good compact postures, free from auto-collisions, we noticed in the last experiment that it may have reachability problem that need to be considered for real environments use. As the ladder inter-stringer width did not allow having both feet on a same rung, the posture in Fig. 1 right image, illustrate that in fact HRP-2 couldn't go touching the rung with the base of the gripper to confirm the contact before closing. For this case we allowed the user to adjust and close the gripper by teleoperation. The reason is simply that the best compact posture to reach the seventh rung with left arm is obtained with left leg and left arm completely stretched, the right one bends with rotating sole and knee nearly in contact with the ladder's run while the CoM can't be put in front further. This suggests that additional length in some links of the arms and legs is welcome. This is what will be done for the next HRP-2 version.

Finally, we considered the possibility to have more dynamical gaits similar to [7]. For instance, by computing the CoM trajectory with a preview of up-coming contact, such as in [19]. This is certainly not necessary since the motion of the robot requires slow motion strategies at contact formation (including grasps) and removal and we do not use hook-like designed grippers.

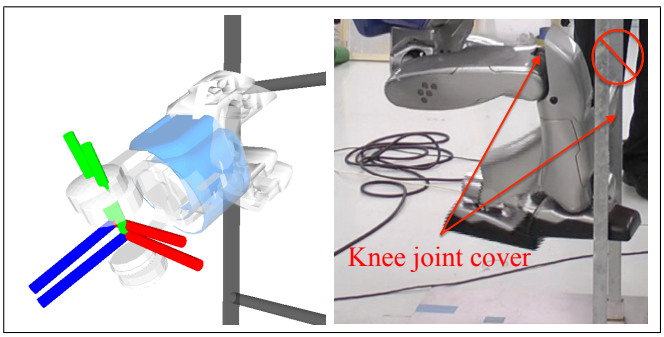

Fig. 9: Tools to assess discrepancies between $\mathbf{q}_{\text{model}}$ and $\mathbf{q}_{\text{estimate}}$. Left leg knee-cover stuck on a rung during left-leg transfer.

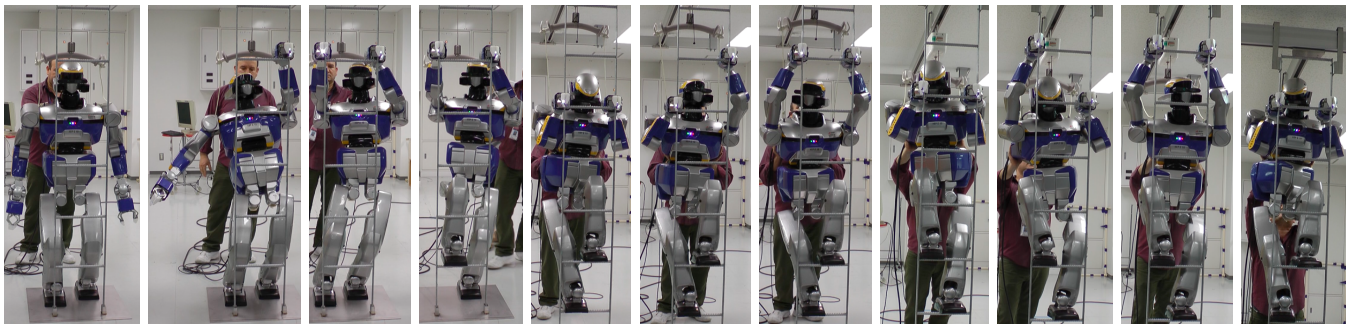

Fig. 7: Ladder climbing with off-line generated trajectories tracked by the low-level joint PD controllers. When needed, adjustments of the grippers positioning is made by the operator (behind the robot). In this experiment, the operator compensates for the lack of firm grasps of the stringers, but not on the lifting power and feet positioning.

Fig. 9(left image) shows tools the correction of the discrepancy due to compliance. However, despite ankle compliance compensation, discrepancies are always present and vision is clearly necessary. There are also additional, less critical issues, that need light hardware or software modifications. However, the one which is to be considered seriously is the situation illustrated in the Fig. 9(right image). In this case, some aesthetic shaping of some parts of the humanoid robot may become a problem. The knee cover in Fig. 9(right image) was stuck on a rung during left leg transfer from ground to the ladder, which resulted in an excess of torques that switched-off the servo. Extra-care shall be taken in designing the cover of the robot so that these situations are avoided.

V. Conclusion

Experiments on different grasping strategies revealed that with a few simple modification, the HRP-2 humanoid robot will be able to fully climb vertical ladders, more details are upcoming in [20]. Its design proved to be efficient in finding good compact postures in order to perform such tasks. However, the current grippers proved to be very limiting since firm grasp capability is the key (as for human) to climb up and down ladders efficiently. Therefore, hardware changes will be performed soon to change the gripper's clamps into new ones that adapt to the grasped ladder's bars, handrails, etc. It is also likely that the arm or leg's length will be increased to avoid cases of kinematic singularities encountered in the some configurations. There is much work to be done for a better robustness of the controller and the planner. Finally, vision must be integrated to our multi-objective controller to achieve visual servoing.

References

[1] Y. Zhang, J. Luo, K. Hauser, R. Ellenberg, P. Oh, H. A. Park, and M. Paldhe, "Motion planning of ladder climbing for humanoid robots," in *IEEE International Conference on Technologies for Practical Robot Applications*, 22-23 April 2013, pp. 1–6.

[2] J. Luo, Y. Zhang, K. Hauser, H. A. Park, M. Paldhe, C. G. Lee, M. Grey, M. Stilman, J. H. Oh, J. Lee, I. Kim, and P. Oh, "Robust ladder-climbing with a humanoid robot with application to the DARPA robotics challenge," in *IEEE International Conference on Robotics and Automation*, HK, China, 31 May - 7 June 2014, pp. 2792–2798.

[3] H. Iida, H. Hozumi, and R. Nakayama, "Developement of ladder climbing robot LCR-1," *Journal of Robotics and Machatronics*, vol. 1, pp. 311–316, 1989.

[4] D. M. Bevly, S. Farritor, and S. Dubowsky, "Action module planning and its application to an experimental climbing robot," in *IEEE International Conference on Robotics and Automation*, San Francisco, CA, 24-28 April 2000, pp. 4010–4015.

[5] H. Nakai, Y. Kuniyoshi, M. Inaba, and H. Inoue, "Metamorphic robot made of low melting point alloy," in *IEEE/RSJ International Conference on Intelligent Robots and Systems*, Lausanne, Switzerland, October 2002, pp. 2025–2030.

[6] S. Fujii, K. Inoue, T. Takubo, Y. Mae, and T. Arai, "Ladder climbing control for limb mechanism robot ASTERISK," in *IEEE International Conference on Robotics and Automation*, Pasadena, CA, USA, 19-23 May 2008, pp. 3052–3057.

[7] H. Yoneda, K. Sekiyama, Y. Hesegawa, and T. Fukuda, "Vertical ladder climbing motion with posture control for multi-locomotion robot," in *IEEE/RSJ International Conference on Intelligent Robots and Systems*, Nice, France, 22-26 September 2008, pp. 3579–3584.

[8] S. Noda, M. Murooka, S. Nozawa, Y. Kakiuchi, K. Okada, and M. Inaba, "Generating whole-body motion keep away from joint torque, contact force, contact moment limitations enabling steep climbing with real humanoid robot," in *IEEE International Conference on Robotics and Automation*, HK, China, 31 May - 7 June 2014, pp. 1775–1781.

[9] K. Bouyarmane and A. Kheddar, "Humanoid robot locomotion and manipulation step planning," *Advanced Robotics*, vol. 26, no. 10, pp. 1099–1126, 2012.

[10] A. Escande, A. Kheddar, and S. Miossec, "Planning contact points for humanoid robots," *Robotics and Autonomous Systems*, vol. 61, no. 5, pp. 428–442, 2013.

[11] K. Bouyarmane, J. Vaillant, F. Keith, and A. Kheddar, "Exploring humanoid robots locomotion capabilities in virtual disaster response scenarios," in *IEEE-RAS International Conference on Humanoid Robots*, Businness Inoovation Center, Osaka, Japan, November 2012.

[12] A. Escande, S. Miossec, M. Benallegue, and A. Kheddar, "A strictly convex hull for computing proximity distances with continuous gradient," *IEEE Transactions on Robotics*, vol. 30, no. 3, pp. 666–678, June 2014.

[13] S. Brossette, A. Escande, J. Vaillant, F. Keith, T. Moulard, and A. Kheddar, "Integration of non-inclusive contacts in posture generation," in *IEEE/RSJ International Conference on Intelligent Robots and Systems*, Chicago, Illinois, 14-18 September 2014.

[14] A. Wächter and L. Biegleri, "On the implementation of an interior-point filter line-search algorithm for large-scale nonlinear programming," *Math. Program.*, vol. 106, no. 1, pp. 25–57, 2006.

[15] F. Kanehiro, M. Morisawa, W. Suleiman, K. Kaneko, and E. Yoshida, "Integrating geometric constraints into reactive leg motion generation," in *IEEE/RSJ International Conference on Intelligent Robots and Systems*, 2010, pp. 4069–4076.

[16] Y. Abe, M. d. Silva, and J. Popović, "Multiobjective control with frictional contacts," in *ACM SIGGRAPH/Eurographics symposium on Computer animation*, 2007, pp. 249–258.

[17] M. d. Lasa, I. Mordatch, and A. Hertzmann, "Feature-based locomotion controllers," *ACM Transactions on Graphics*, vol. 29, no. 4, p. 1, 2010.

[18] K. Bouyarmane and A. Kheddar, "Using a multi-objective controller to synthesize simulated humanoid robot motion with changing contact configurations," in *IEEE/RSJ International Conference on Intelligent Robots and Systems*, San Fransico, CA, 25-30 September 2011, pp. 4414–4419.

[19] H. Audren, J. Vaillant, A. Kheddar, A. Escande, K. Kaneko, and E. Yoshida, "Model preview control in multi-contact motion– application to a humanoid robot," in *IEEE/RSJ International Conference on Intelligent Robots and Systems*, Chicago, Illinois, 14-18 September 2014.

[20] J. Vaillant, A. Kheddar, H. Audren, F. Keith, S. Brossette, K. Kaneko, P. Gergondet, M. Morisawa, E. Yoshida, S. Kajita, and F. Kanehiro, "Multi-contact vertical ladders climbing with the HRP-2 humanoid," *Autonomous Robots*, (submitted).